Available online at www.sciencedirect.com
ScienceDirect
ELSEVIER
Journal of Nuclear Materials 359 (2006) 8–16
journal of nuclear materials
www.elsevier.com/locate/jnucmat

Effect of post-D^+-irradiation time delay and pre-TDS heating on D retention in single crystal tungsten

A.D. Quastel, J.W. Davis, A.A. Haasz *, R.G. Macaulay-Newcombe

University of Toronto Institute for Aerospace Studies, 4925 Dufferin Street, Toronto, ON, Canada M3H 5T6

Received 6 February 2006; accepted 17 July 2006

Abstract

Deuterium retention measurements using thermal desorption spectroscopy were made for single crystal tungsten (SCW) irradiated with D^+ to a fluence of 1×10^{23} D/m^2 at room temperature following various experimental procedures. The dominant desorption peaks in the TDS spectra were at ~400 K and ~600 K, with a peak at ~500 K also present in some cases. The primary findings were (i) D retention was found to decrease by as much as a factor of 2 with increasing the time delay between D^+ irradiation and TDS from <1 h to >8 weeks, indicating the presence of some mobile D in the bulk introduced during irradiation, which could diffuse and escape even at room temperature. (ii) Mild baking of the test chamber to ~360 K between D^+ irradiation and TDS resulted in the escape of ~40% of the trapped deuterium, indicating that additional lower energy traps exist. (iii) Background gas impurities lead to impurity implantation in the near surface of the specimen, which in turn leads to increased trapping of D. However, the effect of impurities on D retention was relatively smaller (about 10–20%) than the effects of mild baking and post-implantation time delay.

© 2006 Elsevier B.V. All rights reserved.

PACS: 28.52.Fa; 79.20.Rf; 61.80.Jh; 61.82.Bg

1. Introduction

The materials selected for plasma-facing components in ITER are beryllium for the chamber walls, carbon for the divertor target plates, where the highest heat loads will occur, and tungsten for the rest of the divertor region [1]. The use of tungsten in fusion devices has generated considerable interest in tungsten's hydrogen trapping characteristics, e.g. [2–4]. While most of the research has involved different forms of polycrystalline tungsten (PCW), several attempts have also been made to separate the effects of various material and experimental parameters. For example, by studying single crystal tungsten (SCW) the trapping of hydrogen in the 'crystal' can be separated from the effects of grain boundaries, dislocations and other defects in the polycrystalline material. However, even in the case of single crystal specimens the presence of inherent defects and impurities and the modification of the material due to the incident H^+ or D^+ will affect hydrogen diffusion and trapping.

To further control the experimental parameters, some studies have been performed at ion implantation energies below the displacement threshold in W

---

* Corresponding author.
E-mail address: tonyhaasz@utias.utoronto.ca (A.A. Haasz).

0022-3115/$ - see front matter © 2006 Elsevier B.V. All rights reserved.
doi:10.1016/j.jnucmat.2006.07.012

(2050 eV for H^+ [5] and 940 eV for D^+ [6]) to prevent the formation of ion-induced damage. Nevertheless, even for energies below the damage threshold, hydrogen accumulation can occur in the material below the surface, extending to depths much greater than the ion range, e.g. [3]. This may cause lattice distortion, and under certain combinations of ion flux, fluence and temperature, it may lead to the formation of vacancy clusters or nano-bubbles [7], microvoids [8,9], and in some cases blistering [10–12] . Clear evidence of blistering has been observed by Haasz et al. [10] in PCW at 500 K for 500 eV/D^+ incident ion energy and fluences above $\sim 10^{24}$ D^+/m^2. Alimov et al. [11] have also seen blisters on PCW at 323 K for 200 eV D^+ energy and ion fluences above $\sim 1 \times 10^{24}$ D^+/m^2, but did not see blisters on SCW surfaces at fluences up to 5×10^{23} D^+/m^2 [11]. However, at much higher fluences ($\sim 1 \times 10^{26}$ D^+/m^2), Tokunaga et al. [12] have observed blisters on SCW at 343 K for 100 eV D^+, but at higher temperatures (383, 623, and 1123 K) no apparent surface modification was seen by SEM [12]. Evidence of blister formation was also reported by Wang et al. [13] for 100 eV/D^+ irradiation of W (type and structure of W was not specified by the authors) at room temperature with a fluence of 10^{25} D^+/m^2.

While it is evident that surface deformation and blistering is more likely to occur at fluences $>10^{24}$ D^+/m^2 for PCW and even higher fluences for SCW (perhaps as high as $\sim 1 \times 10^{26}$ D^+/m^2), there appears to be some inconsistency regarding the temperature at which such effects occur. The question is whether it is only the temperature, or is it possible that the structure and impurities also play a role in causing the varied observations. In the case of PCW it is possible that both the structure and impurities might play a role. However, in SCW structure is not expected to have a significant effect, leaving impurities – both bulk and surface – as possible causes of surface modifications.

Experimental results by Sakamoto et al. for 0.5 keV and 8 keV D_2^+ irradiation cases at room temperature indicated that radiation-induced defects do not strongly influence D retention; they found that residual impurities act as major trapping sites for the implanted D independent of the ion energy [2]. The role of impurities in hydrogen trapping has also been investigated by our group at the University of Toronto [14–16]. Prior to D^+ implantations, specimens were annealed under vacuum at temperatures ranging from 1775 to 2200 K with the intention of reducing the impurity and defect contents. In addition to the presence of impurities in the bulk, impurities originating from the background gas during D^+ irradiation were also found to affect the level of deuterium retention [14,15]. Reduction of the impurity levels (H_2O, CO_2, etc.) in the background gas during D^+ implantation led to reductions in the amount of trapped deuterium [15]. It was proposed that recoil implantation of carbon and oxygen impurities arriving at the surface from the gas phase created vacancies in tungsten, thereby increasing D trapping [15].

The current experiments were undertaken with the objective to further investigate how exposure to background impurities during the various stages of the experiment (implantation, post-implantation, and thermal desorption) might affect the measured amount of deuterium released from the specimen during desorption. In the previous experiments [14–16] thermal desorption spectroscopy (TDS) was performed in a separate vacuum chamber, necessitating specimen transport in air. Although it is not likely that surface adsorption due to air exposure would have affected the amount of D released from the specimen during TDS, the ‘mild’ baking of the TDS chamber prior to desorption (~410 K for 2 h to reduce the background pressure [15,16]) and the time delay between implantation and TDS (typically, 8 h to several days) might have led to some D losses of mobile and weakly trapped D. For the current study, the implantation chamber was modified to allow post-implantation TDS to be performed in the implantation chamber, allowing for control of the time delay without exposing the specimen to air.

2. Experiment

2.1. Specimens

The single crystal tungsten used for this study was produced by the Rare Metals Institute in Moscow. The quoted purity was 99.98 wt% where the primary impurities were H (≈0.02 at.%), C (≈0.05 at.%), N (≈0.01 at.%), and O (≈0.05 at.%). Six specimens were diamond cut into 5×5 mm^2 rectangles from a disc of 25 mm diameter and ~0.7–0.9 mm thickness. The specimen surface normal vector was measured by orientation imaging spectroscopy to be within 15 degrees of the [0 0 1] crystallographic direction [15]. The specimen surface preparation procedure followed by Poon et al., e.g. [14–16] was further developed to improve the resulting surface finish. The modified procedure included: a mechanical polish to remove all traces of previous implantations (removal of ∼10–100 μm), followed by an anneal in vacuum to 1750–1800 K for about 15 min, then an electropolish conducted in a high purity electrolyte, and finally a second anneal in vacuum at 1750 K for about 5 min. This procedure produced very smooth surfaces with surface roughness of 10–20 nm, as measured with an interferometer, but more importantly, these surface finishes were highly reproducible.

Prior to D^+ ion implantations every specimen was thermally annealed, for a third time, at 1750–1800 K. This anneal temperature is less than half the melting temperature of tungsten (3680 K), so it is unlikely that point defects or dislocations will be removed entirely, especially from the bulk [14]. However, the temperature is high enough to remove any electropolish residue from the surface, as well as impurities, vacancies and dislocations from the near surface that were not removed by the electropolish, and also to reduce the dislocation content in the bulk [7,17].

2.2. Apparatus

To conduct specimen annealing, D^+ implantation, and TDS in the same vacuum chamber, without breaking vacuum, the specimen holder and heating apparatus were designed to enable (i) specimen heating away from the ion beam aperture, and (ii) specimen positioning in front of the ion beam aperture for D^+ implantation.

An electron gun heater, consisting of a resistively-heated tungsten filament, an aperture plate, and housing, was used to heat the specimen during annealing and TDS. A rhenium–tungsten thermocouple was spot welded to one corner of the specimen to measure its temperature during annealing and TDS. The specimen heating system employed feedback from the thermocouple to control the current to the electron gun filament. With the specimen biased to 6.5 kV, high voltage isolation circuitry was required for measuring the thermocouple signals and enabling computer monitoring and control of the specimen temperature. Heating rates within ±7% of desired value were normally achieved during annealing and TDS.

Movement of the specimen holder was achieved with the use of an *X*–*Y*–*Z* motion device. During heating, the holder was positioned in front of the electron gun, and the beam aperture heat shield (with the beam stop attached to it) was swiveled in front of the ion beam aperture as shown in Fig. 1(a). The beam stop was used for measuring the beam current and conditioning the ion beam prior to D^+ implantation. The stainless steel heat shield was used to reduce the heat load on the beam aperture generated by the specimen during TDS (i.e., to prevent the release of any implanted D in the ion beam aperture plate). During D^+ implantation, the heat shield/beam stop assembly was swiveled out of the way of the D^+ beam and the specimen was moved in front of the beam aperture; see Fig. 1(b). This experimental configuration allowed the beam current to be monitored before and during D^+ implantations.

2.3. D^+ irradiation/implantation

All of the D^+ implantations were performed in our ultra-high vacuum single-beam accelerator facility using D_3^+ ions at normal incidence to the test specimen. In order to generate large flux densities, 2.5 keV D_3^+ ions were used, with the specimen biased to +1 kV to decelerate the ions, resulting in 500 eV/D^+ energy. (We denote the incident particle as D^+, although not all of the D particles are charged in the D_3^+ ion.) Beam fluxes through a 2 mm diameter aperture were in the range 7×10^{19}–1.1×10^{20} D^+/m^2 s. A fluence of 1×10^{23} D^+/m^2 was used in all experiments; this fluence is on the saturation segment of the D retention curve for SCW [18]. Fluence variations from experiment to experiment were kept <10%. All implantations were performed with the specimen at room temperature. The gas composition in the test chamber during implantations was monitored with a quadruple mass spectrometer (QMS).

To achieve very low background pressures (1–5×10^{-7} Pa), the test chamber and some upstream components of the accelerator were baked at ∼470 K for 18–24 h prior to D^+ implantations. In most experiments an additional reduction of the condensable impurity species in the background gas (e.g., hydrocarbons, water, and carbon dioxide) was achieved by incorporating a liquid nitrogen ($LN_2 \sim 80$ K) cooling line on the beam aperture mounting plate, near the specimen (see Fig. 1). For some experiments, which will be explicitly noted, the test chamber was further baked at ∼360 K following D^+ implantation, but before TDS. This heating step was used to investigate

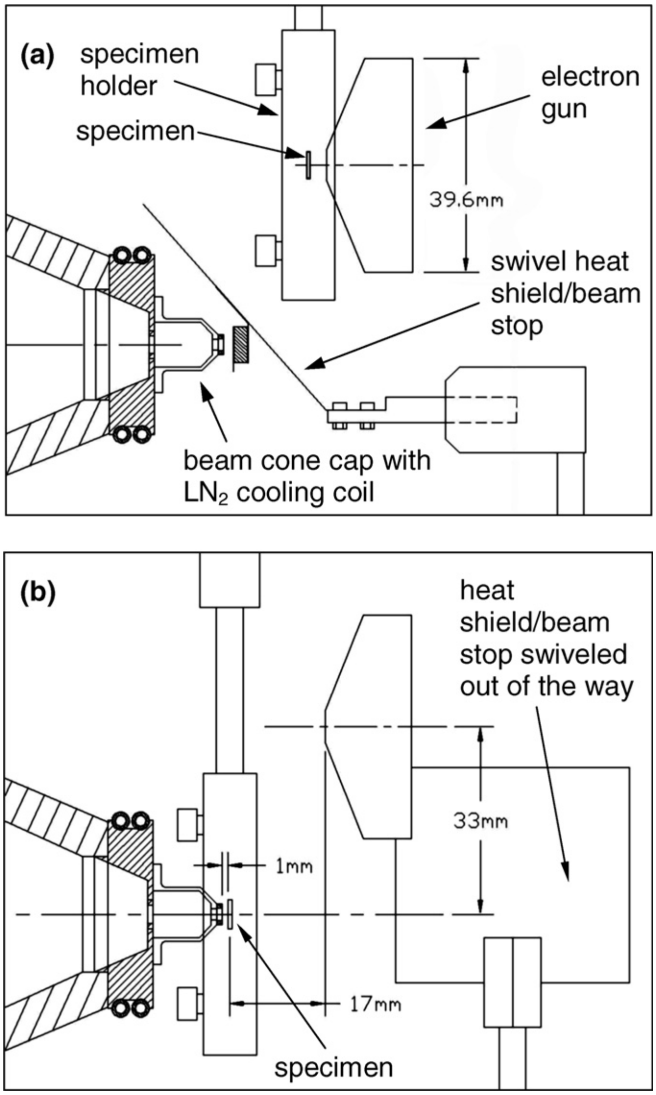

Fig. 1. Schematic of apparatus showing the specimen holder assembly and electron gun used for specimen annealing and TDS. (a) Specimen positioned in front of the electron gun for anneal/TDS. (b) Specimen in front of the 2 mm diameter ion beam aperture for D^+ irradiation.

the presence of mobile and/or weakly trapped deuterium.

2.4. Thermal desorption spectroscopy (TDS)

For most of the specimens, except #15A and #16A, TDS was performed in the implantation chamber without exposing the specimens to air after implantation. During TDS the specimen was positioned in front of the electron gun and was heated by electron bombardment. For most cases, except #15A and #16A, the temperature was increased at a constant ramping rate of 5–5.5 K/s to ~1750 K, where it was held for 5 min. The ramping rates for #15A and #16A were lower than for the other specimens (3.1 and 3.4 K/s, respectively) due to constraints associated with the separate TDS chamber [16].

The released gas species were measured with a Hiden QMS (model HAL IV RC PIC) which was set to scan, once per second, the masses 2, 3, 4, 18, 20, 28, 32, and 44, corresponding to H_2, HD, D_2, H_2O, D_2O, $CO + N_2$, O_2, and CO_2, respectively. A calibration D_2 leak bottle connected to the test chamber was used for calibrating the QMS. The test chamber pressure with the leak bottle off was typically $\sim 6 \times 10^{-7}$ Pa and with the leak bottle on it was $\sim 1.6 \times 10^{-6}$ Pa (mainly D_2). During D^+ implantation the chamber pressure was $\sim 9 \times 10^{-6}$ Pa, and during TDS the pressure increased to $\sim 6 \times 10^{-5}$ Pa.

2.5. SIMS

A time-of-flight secondary ion mass spectroscopy facility at the Department of Chemical Engineering, University of Toronto, was used to measure near surface concentrations of various elements in the SCW specimens. The analysis beam was 2.5 keV Ga^+ with 2.4 pA over (50 μm)^2 area. The sputter beam used for depth profiling was 1 keV Cs^+, with 8.4 nA over (200 μm)^2 area. SIMS was used to obtain depth distributions (within 2–60 nm) of H^-, D^-, C^-, O^-, and tungsten oxides: $^{183}WO_2^-$, $^{183}WO_3^-$, $^{184}WO_2^-$, and $^{184}WO_3^-$.

3. Results and discussion

All of the experimental results presented here were performed with newly polished (virgin) SCW specimens following the surface preparation described in Section 2.1. Ion implantation was performed with a 1.5 keV D_3^+ (i.e., 500 eV/D^+) beam of $\sim 1 \times 10^{20}$ D^+/m^2s flux and $\sim 1 \times 10^{23}$ D/m^2 fluence. The controlling parameters in the experiments were (i) the time delay between D^+ implantation and TDS; (ii) whether LN_2 cooling was used to suppress background gas impurities; (iii) whether the specimen was in vacuum or in air during the time delay; and (iv) whether mild baking (~360 K) of the vacuum chamber, with the specimen in it, was performed prior to TDS. The experimental conditions, as well as the measured retained fluences, are summarized in Table 1. Each experiment was assigned a number which identifies the sequence of experimental runs. The runs are grouped to reflect commonality in some of the above controlling parameters. For example, runs #11, 13, and 19 had no LN_2 beam aperture cooling, no air exposure and no mild baking before TDS, but the post-implantation time delays were different.

3.1. Effect of reduced background impurities by using LN_2 aperture cooling

In the following experiments three specimens (runs #11, 13, 19) were irradiated without LN_2 beam aperture cooling. Here the deuterium retention values were within ~2% of each other and averaged 7.8×10^{20} D/m^2; see Table 1 and Fig. 2 where

Table 1
Summary of controlling experimental conditions and the measured D retention

Experiment (Run #)	LN_2 beam aperture cooling used	In air before TDS	Mild bake before TDS	Time delay before TDS (h)	Retained amount (10^{20} D/m^2)	Ramp rate during TDS (K/s)	Comments
11	No	No	No	0.42	7.9	5.5	
13	No	No	No	0.18	7.7	5.2	
19	No	No	No	0.72	7.8	5.6	
12	Yes	No	No	0.42	5.9	6.4	
15	Yes	No	No	0.37	6.3	5.1	
16	Yes	No	No	21.5	6.2	5.0	
17	Yes	Yes	Yes: 360 K (5 h)	63	3.7	5.1	Time delay includes 18 h in air
21	Yes	No	Yes: 360 K (5 h)	71	3.9	5.2	Time delay totally in vacuum
15A	Yes	Yes	No	1848 (11 weeks)	3.2	3.1	SIMS performed before TDS (6–8 weeks after D^+)
16A	No	Yes	No	1344 (8 weeks)	3.5	3.4	SIMS performed before TDS (3–5 weeks after D^+)
Poon et al. [14]	Yes*	Yes	Yes: 400 K	8–24 h (avg: 16 h)	3.8		For comparison purposes
Haasz et al. [18]	No	Yes	No	>12	4.5		For comparison purposes

* LN_2 cooling involved the use of an 'LN_2 cold finger' [14].

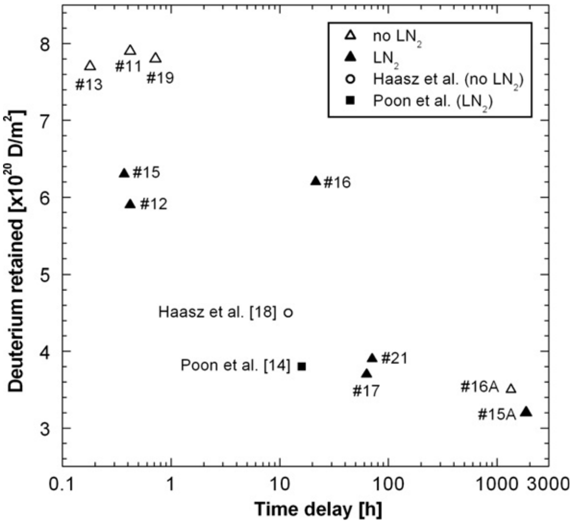

Fig. 2. D retention as a function of time delay between D$^+$ implantation and TDS. Experimental run numbers are shown beside the data points. Implantation fluence: 1×10^{23} D/m^2; specimen temperature during implantation: 300 K.

the total amount of retained D is plotted as a function of the time delay between irradiation and TDS. The relatively small time delay range for these three cases (0.18–0.72 h) did not appear to affect the total amount of retained D – more on this in Section 3.2. The TDS profiles corresponding to these runs are characterized by two prominent peaks: at 400 and 600 K; see Fig. 3(a). These three experiments yielded the highest retention levels obtained in the present study.

In a second set of experiments (runs #12, 15, 16), LN$_2$ cooling was used to cool the beam aperture and part of the beam line to temperatures ~80 K, resulting in the following QMS signal reductions in the background gas: mass 18 (H_2O): >50%, mass 28 ($CO + N_2$): >55% and mass 44 (CO_2): ~70%. TDS results for these specimens gave D retention levels which were within 7% of each other, with an average of 6.2×10^{20} D/m^2 demonstrating good reproducibility; see Table 1 and Fig. 2. It is clearly evident that the reduction of background impurities due to LN$_2$ cooling has led to a reduction of ~20% in total D retention. As with the #11–13–19 cases, the total retention levels were not affected by the time delays, which ranged from 0.42–21.5 h; see Section 3.2 for further discussion. The TDS spectra for #12–15–16 (Fig. 3(b)) are characterized by a primary peak at 600 K which is comparable to the non-LN$_2$-cooling cases. However, the peak at 400 K is considerably reduced with LN$_2$ cooling, and a shoulder indicative of a possible peak at ~500 K appears.

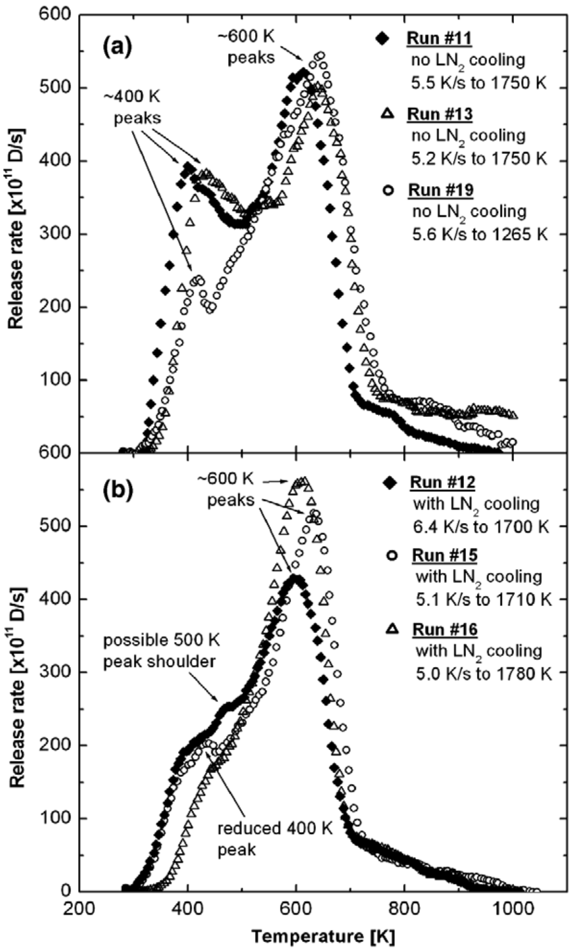

Fig. 3. TDS spectra for implantation fluence of 1×10^{23} D/m^2 and 300 K specimen temperature: (a) without LN$_2$ cooling of the ion beam aperture, and (b) with LN$_2$ cooling.

Two further specimens (runs #15A and 16A) were implanted with 1×10^{23} D/m^2 for subsequent SIMS analysis. LN$_2$ cooling was used in run #15A, but not in #16A. For these specimens, after prolonged air exposure (1848 h for #15A and 1344 h for #16A), TDS was conducted in a different vacuum chamber, the one used by Poon et al. [15,16]. Two key observations are noted in Table 1 and Fig. 2: (i) the reduction of total D retention due to LN$_2$ cooling is relatively smaller (~10% compared to ~20% observed above), and (ii) the total amount of retained D is substantially lower (about a factor of 2) compared to levels seen in experiments where the time delay is relatively short and the specimen is kept in vacuum. This would indicate a time delay effect which is discussed in Section 3.2.

3.2. Effect of post-implantation time delay

For specimens #12–15–16 implanted with LN_2 cooling some differences are observed in the TDS spectra; see Fig. 3(b). For #12 and #15 where the delay times were 0.42 and 0.37 h, respectively, the D desorption begins at ~300 K – the D^+ implantation temperature. However, in run #16, where the time delay was increased to 21.5 h, the D release begins at a higher temperature (~350 K), indicating that some weakly trapped D has been slowly escaping from the specimen, or has been transferred to higher energy trapping sites.

As noted above, the specimens that were used for SIMS profile analysis (#15A and #16A) also showed a time dependent D release, but to a greater degree. TDS for these specimens was performed several weeks after D^+ implantation, during which time they were stored in air. From Fig. 4(a) we note that desorption of D from both specimens begins at ~400 K. Two distinct desorption peaks, at ~500 and ~600 K, are present, consistent with previous measurements [14,15,18], but no 400 K peak is observed. Also, the desorption ends abruptly at around 700 K and the profiles do not show the prominent tail section (usually terminating at ~1000 K) seen earlier in the experiments without long post-implantation time delays; compare Fig. 4(a) with Fig. 3(a) and (b). The absence of D release at <400 K and >700 K in the desorption spectra is consistent with the observed significant reductions (about a factor of 2) in the total amount of D retention, as noted in Section 3.1.

3.3. Effect of post-implantation mild baking

The retention results presented above for cases with and without LN_2 cooling, except for the very long time delay runs (#15A and #16A), were higher than those measured previously by Poon et al. [14,16,18]. For example, the present retention levels without LN_2 cooling are about a factor of two higher than reported in [14,16]. The key difference in the present and previous [14–16] experimental procedures is the combination of air exposure and pre-TDS mild baking of the TDS chamber in [15] and the absence of these steps in the present study for runs #11–13–19 and #12–15–16.

To study the effect of air exposure and mild baking, two specimens were implanted using LN_2 cooling and TDS was performed in the implantation chamber. In the 1st experiment (run #17) the specimen was exposed to air at atmospheric pressure for 18 h after D^+ implantation and then in vacuum for another 45 h, for a total time of 63 h before TDS was performed. For the second experiment (run #21) the test chamber remained in vacuum throughout the whole procedure, with a time delay of 71 h. For both experiments a mild bake (at ~360 K) of the implantation/TDS chamber (same chamber in these experiments) was conducted for 5 h and then

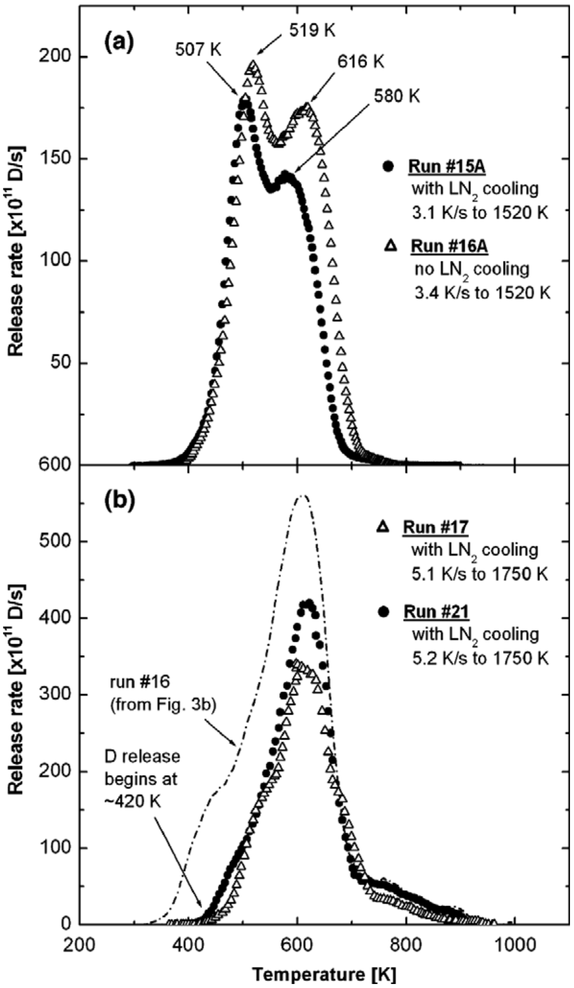

Fig. 4. TDS spectra for implantation fluence of 1×10^{23} D/m^2 and 300 K specimen temperature. (a) These specimens were prepared for SIMS and prior to SIMS they were exposed to atmosphere for 8–11 weeks. Run #15A was obtained with and run #16A without LN_2 cooling. TDS for these specimens was done in a separate vacuum chamber. (b) Runs #17 and #21 were both obtained with LN_2 cooling and also with mild baking (~360 K) of the implantation chamber where TDS was performed; however, #17 was exposed to air prior to TDS while #21 was not. The TDS spectrum for run #16 which was also obtained with LN_2 cooling, but without mild baking, is shown for comparison.

the chamber was allowed to cool before TDS. Desorption spectra for these two cases are almost identical, with one dominant peak at ∼600 K; see Fig. 4(b). In both cases the mild baking has resulted in the complete elimination of the peak at ∼400 K, leaving only a barely discernible shoulder. The comparison of the #17 and #21 profiles with that of run #16, where no mild baking but LN_2 cooling was used, strongly suggests that some deuterium has escaped during the mild bake procedure. The retained D for #17 and #21 is $\sim(3.7–3.8) \times 10^{20}$ D/m^2 compared with $\sim 6.2 \times 10^{20}$ D/m^2 for #16, corresponding to a D loss of ∼40%; see Table 1 and Fig. 4(b). However, the wait in atmosphere in run #17 did not substantially affect the measured D retention compared to run #21, where the wait period occurred under vacuum. The D retention values for #17 and #21 are within ∼5%, again indicating excellent experimental reproducibility; compare the retained D in Table 1 and the 600 K peaks for #17 and #21 in Fig. 4(b). These D retention values are in general agreement with the values measured by Poon et al. for experiments with mild baking at ∼400 K, e.g. [14]. These experiments indicate that it is the mild baking procedure which has led to the differences in the retention levels between the current experiments and those of Poon et al. [14,16,19]. Air exposure prior to TDS appears to have a negligible effect.

3.4. SIMS surface analysis of specimens

To investigate the effect of molecular background impurities in the implantation chamber, such as H_2O, CO_2, CO, O_2 and various hydrocarbons, on D retention in SCW, SIMS analysis was performed on two irradiated specimens: #15A with LN_2 cooling and #16A without LN_2. In both cases no post-implantation TDS was performed prior to SIMS analysis, but TDS was eventually performed. On #15A SIMS was performed ∼7 weeks (∼1180 h) and for #16A ∼4 weeks (∼670 h) after D^+ implantation. Fig. 5 shows eight curves representing the depth profiles for D, C, O, and $^{184}WO_2$ with and without LN_2 cooling during D^+ implantation. Deuterium, carbon, oxygen, and $^{184}WO_2$ levels are all consistently higher for the case where LN_2 cooling was not used. Furthermore, SIMS analysis showed that noticeable decreases in the levels of O and C atoms were accompanied with a decrease in the retained D in the first 40 nm depth in the specimens. These observations are consistent with the hypothesis suggested by Poon et al. [15] that background gas impurities are driven into the specimen via recoil implantation, and consequently, the implanted impurities (mainly O) lead to increased D retention [15,16]. Subsequent to SIMS analysis, TDS was performed for both specimens as discussed above.

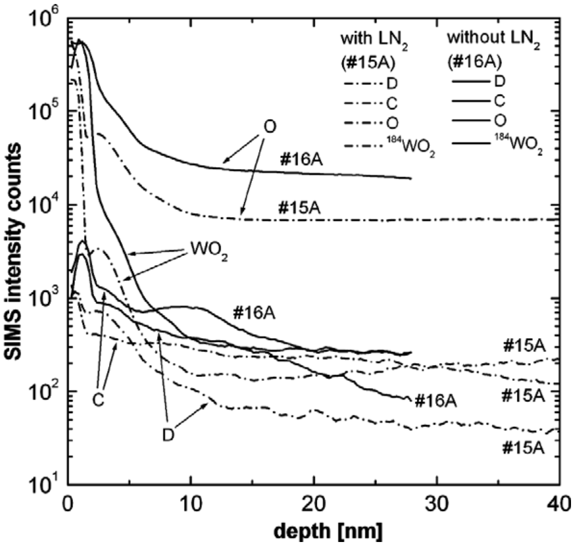

Fig. 5. SIMS depth profiles for specimens #15A and #16A irradiated with a fluence of 1×10^{23} D/m^2 at 300 K obtained prior to TDS. LN_2 cooling was used for #15A, but not for #16A.

4. Summary and conclusions

4.1. Deuterium retention

Deuterium retention levels obtained in the present study where D^+ implantation and TDS was performed within <1 h (for the most part) in the same chamber, without breaking vacuum, were found to be about 60–120% higher than previous measurements [14,16,18] that employed a procedure where the specimen was exposed to air between D^+ implantation and TDS, the time delay between D^+ implantation and TDS was >8 h, and the TDS chamber containing the specimen was baked at ∼410 K prior to TDS.

4.2. Desorption spectra

TDS spectra in the present study had dominant desorption peaks at ∼400 K and ∼600 K, with a peak at ∼500 K also present in some cases. By comparison, previous TDS results [16] show dominant peaks at ∼500 K and ∼600 K – but no peak at 400 K. From previous TMAP modelling of D trapping in W [16] the observed desorption peaks at 500 and 600 K were found to correspond to trapping energies of ~1.2 eV and ~1.4 eV, respectively. More recent modelling with the updated multi-trap TMAP-7 code [19] by Poon et al. have also yielded similar trapping energies for the 500 and 600 K peaks and a trapping energy of about 0.65 eV for the 400 K peak [20].

4.3. Effect of mild baking

It was found that subsequent to D^+ implantation, mild baking of the test chamber to ~360 K resulted in the escape of ~40% of the trapped D. The loss of this weakly-trapped deuterium corresponds to the near elimination of the ~400 K peak as well as a reduction in the total amount of D retained. This leads to the conclusion that additional lower energy traps exist, containing about ~40% of the trapped D.

4.4. Effect of post-implantation time delay

Thermal desorption performed >8 weeks after D^+ irradiation has led to about a factor of 2 reduction in total D retention compared with the <1 h time delay cases. This indicates that during D^+ irradiation some mobile D diffuses deep into the bulk, requiring relatively long post-irradiation times at room temperature to diffuse to the surface and be released. The tail of the desorption profile between 700 and 1000 K was eliminated by this time delay.

4.5. Effect of impurities

The present results, in agreement with previous results [15], show that background gas impurities lead to impurity implantation in the near surface of the specimen, which in turn leads to increased trapping of D. This is consistent with the hypothesis of recoil implantation of surface adsorbed O and C into the sub surface during D^+ irradiation [15,16]. However, the effect of impurities on D retention was relatively smaller than the effects of mild baking and post-implantation time delay.

Acknowledgements

The funding from the *Natural Sciences and Engineering Research Council* of Canada is gratefully acknowledged. We thank Dr V.Kh. Alimov for providing the SCW material and Peter Brodersen at the *University of Toronto Chemical Engineering Department* for performing the SIMS analysis. We also thank Daniel Gelbart who provided technical advice in designing the high voltage isolation circuitry and Charles Perez for his careful work in fabricating many parts of the apparatus.

References

[1] G. Federici, C.H. Skinner, et al., Nucl. Fusion 41 (2001) 1967.
[2] R. Sakamoto, T. Muroga, N. Yoshida, J. Nucl. Mater. 233–237 (1996) 776.
[3] A. A Haasz, J.W. Davis, M. Poon, R.G. Macaulay-Newcombe, J. Nucl. Mater. 258–263 (1998) 889.
[4] R.A. Causey, T.J. Venhaus, Phys. Scripta T 94 (2001) 9.
[5] R. Sakamoto, T. Muroga, N. Yoshida, J. Nucl. Mater. 220–222 (1995) 819.
[6] K. Tokunaga, M. Takayama, T. Muroga, N. Yoshida, J. Nucl. Mater. 220–222 (1995) 800.
[7] H. Eleveld, A. van Veen, J. Nucl. Mater. 212–215 (1994) 1421.
[8] V.Kh. Alimov, K. Ertl, J. Roth, K. Schmid, Phys. Scripta T 94 (2001) 34.
[9] R.G. Macaulay-Newcombe, A.A. Haasz, M. Poon, J.W. Davis, in: Proceedings of the NATO Advanced Research Workshop on Hydrogen Isotope Recycling at Plasma-Facing Materials in Fusion ReactorsNATO Science Series II: Mathematics, Physics and Chemistry, vol. 54, Kluwer Academic Publishers, Dordrecht, 2002, p. 145.
[10] A.A. Haasz, M. Poon, J.W. Davis, J. Nucl. Mater. 266–269 (1999) 520.
[11] V.Kh. Alimov, J. Roth, M. Mayer, J. Nucl. Mater. 337–339 (2005) 619.
[12] K. Tokunaga, M.J. Baldwin, et al., J. Nucl. Mater. 337–339 (2005) 887.
[13] W. Wang, J. Roth, S. Lindig, C.H. Wu, J. Nucl. Mater. 299 (2001) 124.
[14] M. Poon, A.A. Haasz, J.W. Davis, R.G. Macaulay-Newcombe, J. Nucl. Mater. 313–316 (2003) 199.
[15] M. Poon, R.G. Macaulay-Newcombe, J.W. Davis, A.A. Haasz, J. Nucl. Mater. 337–339 (2005) 629.
[16] M. Poon, Deuterium trapping in tungsten, PhD Thesis, University of Toronto, 2004.
[17] R.A. Anderl, D.F. Holland, et al., Fus. Technol. 21 (1992) 745.
[18] A.A. Haasz, M. Poon, R.G. Macaulay-Newcombe, J.W. Davis, J. Nucl. Mater. 290–293 (2001) 85.
[19] G.R. Longhurst, TMAP-7, TMAP-7 user Manual, Idaho National Laboratory, INEEL/EXT-04-02352 (2004).
[20] M. Poon, A.A. Haasz, J.W. Davis, J. Nucl. Mater., to be published.